NJC

PAPER

View Article Online
View Journal | View Issue

Cite this: *New J. Chem.*, 2019, **43**, 4518

Photophysical properties and photodynamic therapy activity of a *meso*-tetra(4-carboxyphenyl)porphyrin tetramethyl ester–graphene quantum dot conjugate†

Muthumuni Managa, * Bokolombe Pitchou Ngoy and Tebello Nyokong *

Received 6th December 2018,
Accepted 16th February 2019

DOI: 10.1039/c8nj06175k

rsc.li/njc

Novel *meso*-tetra(4-carboxyphenyl)porphyrin tetramethyl ester metal derivatives were synthesised and characterized. These derivatives were interacted with graphene quantum dots (GDQs). Spectroscopic evidence that was obtained showed that the resultant conjugates were stable due to the strong π–π stacking interaction between the GQDs and the porphyrins. The fluorescence and singlet oxygen generating behaviour of the porphyrins and the nanoconjugates were investigated following incorporation. The dark toxicity and photodynamic therapy activities of the porphyrins and the nanoconjugates were successfully studied using MCF-7 breast cancer cells. Cell viability for the dark toxicity was more than 90% for all complexes. The PDT activities at the highest concentration of 120 μg ml^{-1} showed a decrease in cell viability down to 15.2% for the GaClTMPP–GQDs.

Introduction

There has been great interest in improving cancer treatments due to high morbidity and mortality that is often associated with this disease. Among the emerging cancer therapies, photodynamic therapy (PDT) surpasses the traditional methods, which include surgery, chemotherapy and radiotherapy.[1,2] The advantages of PDT over traditional methods are that it is non-invasive in nature, has fewer side effects, causes negligible drug resistance and has low systemic toxicity.[1–4]

PDT is a process that requires a combination of laser light with an appropriate wavelength, a photosensitizer (PS), and molecular oxygen[5,6] to elicit a therapeutic response. The production of singlet oxygen has been reported to depend on the triplet state population and the effectiveness of the energy transfer process between the excited triplet state of the photosensitizer and ground state molecular oxygen.[7] The electronically excited photosensitizer transfers its energy to the ground state molecular oxygen to produce an excited singlet oxygen, which acts as the chief cytotoxic species[6,8] in PDT.

Porphyrins have received great attention as the first and second generation of PS[9] because of their effective singlet oxygen ($^1O_2$) generation ability, low toxicity and aromaticity.[10–12] However, their poor physicochemical stability, hydrophobic property and low cell-uptake efficiency limit their widespread application in biomedicine. Various nanocarriers have been actively developed for porphyrins in order to enhance their physicochemical applications[13–15] where cellular uptake has limited their broad application; an example of one of these nanocarriers is graphene quantum dots (GQDs).

GQDs are known to have excellent optical and electronic properties coupled with high photostability, aqueous solubility and bio-compatibility.[16,17] These properties have made GQDs very attractive as alternatives to semiconductor QDs for applications in fluorescence bio-imaging, sensing (biosensors and chemosensors), photocatalysis, drug delivery and as photosensitizers in photodynamic therapy (PDT).[18–21]

GQDs are well known PDT agents with high singlet oxygen quantum yields.[21] Hence, combining the two PDT agents (porphyrins and GQDs) is expected to improve the PDT through a synergistic effect. *meso*-Tetra(4-carboxyphenyl)porphyrin tetramethyl ester has been reported before[22] but we report for the first time the GaCl and Zn derivatives as well as the photophysical behaviour of *meso*-tetra(4-carboxyphenyl)porphyrin tetramethyl ester and metal derivatives non-covalently linked to GQDs. Ester-containing porphyrins are known PDT agents,[8] hence an ester containing porphyrin is employed in this work. The presence of delocalized π electrons facilitates the interaction of porphyrins with GQDs through non-covalent π–π stacking.

Experimental

Materials and methods

Zn tetraphenyl porphyrin (ZnTPP), gallium chloride and zinc chloride were purchased from Sigma-Aldrich. Dichloromethane

Centre for Nanotechnology Innovation, Department of Chemistry, Rhodes University, Grahamstown 6140, South Africa. E-mail: m.managa@ru.ac.za, t.nyokong@ru.ac.za; Fax: +27 46 6225109; Tel: +27 46 6038260/8801

† Electronic supplementary information (ESI) available: Equipment used, procedure for *in vitro* dark toxicity and PDT, photochemical and photophysical parameters, NMR spectra of TMPP and mass spectra of TMPP, GaClTMPP and ZnTMPP. See DOI: 10.1039/c8nj06175k

(DCM), dimethyl sulfoxide (DMSO) and dimethylformamide (DMF) were purchased from Merck. All other reagents and solvents were obtained from commercial suppliers and used as received. Graphene quantum dots (GQDs) were synthesized following the procedures reported elsewhere[23] and the conjugation of the porphyrins to the GDQs was as previously described.[19] The metal-free *meso*-tetra(4-carboxyphenyl)porphyrin tetramethyl ester (TMPP) was synthesized as reported before.[22]

The MCF-7 breast cancer cells were obtained from Cellonex. Dulbecco's phosphate-buffered saline (DPBS) and Dulbecco's modified Eagle's medium (DMEM) were obtained from Lonza, 10% (v/v) heat-inactivated fetal calf serum (FCS), and the 100 mg ml^{-1}-penicillin–100 unit per ml-streptomycin–amphotericin B mixture were obtained from Biowest®, and octanol was obtained from SAARCHEM.

Equipment employed in this work as well as the procedure for the *in vitro* dark toxicity and PDT can be found in the ESI.†

Synthesis

Metallo porphyrins, Scheme 1. In a two-necked flask, DMF was brought to reflux temperature while stirring and then, TMPP (0.1 g, 1.18 mmol) was added and the temperature was brought to 100 °C. Then, zinc chloride (0.05 g, 0.36 mmol) or gallium chloride (0.05 g, 0.28 mmol) was added and the mixture was heated continously for 15 min. The completion of the reaction was checked using a UV/Vis spectrophotometer. The reaction vessel was then allowed to cool to room temperature. DMF/water mixture (30 ml) was added to the resulting product to precipitate the metallated porphyrin, and then the product was filtered off and washed and then air dried.

ZnTMPP. Yield: (21%) UV/Vis (DMF) λ_{max} nm (log ε): 422 (4.51), 559 (3.94), 598 (3.65). ^{1}H NMR (600 MHz, $CDCl_3$) δ 8.84 (s, 8H), 8.46 (d, J = 7.5 Hz, 8H), 8.31 (d, J = 7.5 Hz, 8H), 4.13 (s, 12H) ppm. Calc. for $C_{52}H_{36}N_4O_8Zn$: C = 68.61, H = 3.99, N = 6.16, found: C 68.59, H = 3.97, N = 6.15 MALDI-TOF-MS m/z calc.: 910.24. Found $(M + H)^+$ 911.07.

GaClTMPP. Yield: (19%) UV/Vis (DMF) λ_{max} nm (log ε): 422 (4.51), 559 (3.94), 598 (3.65). ^{1}H NMR (600 MHz, $CDCl_3$) δ 8.82 (s, 8H), 8.47 (d, J = 7.5 Hz, 8H), 8.33 (d, J = 7.5 Hz, 8H), 4.15 (s, 12H) ppm. Calc. for $C_{52}H_{36}N_4O_8Ga$: C = 68.29, H = 3.97, N = 6.13, found: C 68.20, H = 3.96, N = 6.11 MALDI-TOF-MS m/z calc.: 950.05. Found $(M–Cl)^+$ 914.55.

Self-assembly, Scheme 2. The non-covalent coordination (π–π stacking) of GQDs with the metal-free *meso*-tetra(4-carboxyphenyl)porphyrin tetramethyl ester and the metal derivatives was achieved following a method employed before.[19] The presence of delocalized π electrons facilitates the interaction of GQDs with porphyrins through non-covalent π–π stacking. The nanocomposites are represented as TMPP–GQDS, ZnTMPP–GQDs and GaClTMPP–GQDs.

Results and discussion

Characterization of the porphyrin–GQD conjugates

The syntheses of GaClTMPP and ZnTMPP are shown in Scheme 1. The complexes were characterized by elemental analyses, NMR, IR, and MALDI-TOF mass spectroscopy. The obtained data were consistent with the predicted structure. The representation of the nanocomposites of GQDs and the porphyrins *via* π–π stacking are shown in Scheme 2.

UV-Vis spectra

The ground state electronic absorption spectra of porphyrins are characterized by an intense band called the Soret or B band at about 400 nm and the Q bands are observed between 500 and 600 nm. These porphyrin phenomena are explained by the Gouterman's four-orbital model.[24] In this model, the two highest occupied molecular orbitals (HOMOs), the a_{1u} and a_{2u} and lowest unoccupied molecular orbitals (LUMO), the degenerate e_g are taken into account.[25]

The Soret bands of TMPP and TMPP–GQDs are observed at 419 nm, and an additional peak is observed for the TMPP–GQDs

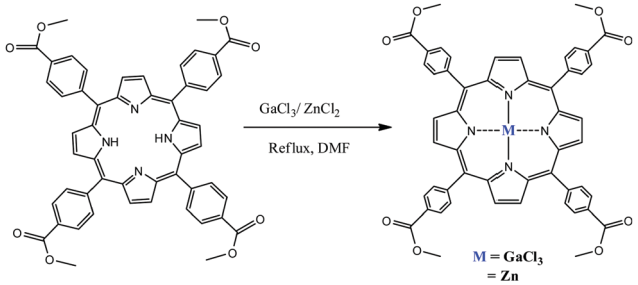

Scheme 1 Metal insertion into metal free *meso*-tetra(4-carboxyphenyl)-porphyrin tetramethyl ester.

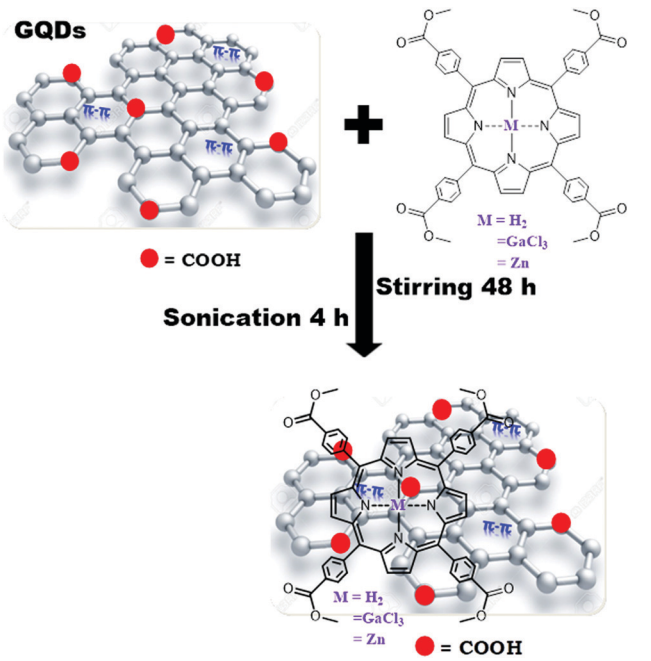

Scheme 2 Representation of the interaction between porphyrins and GQDs.

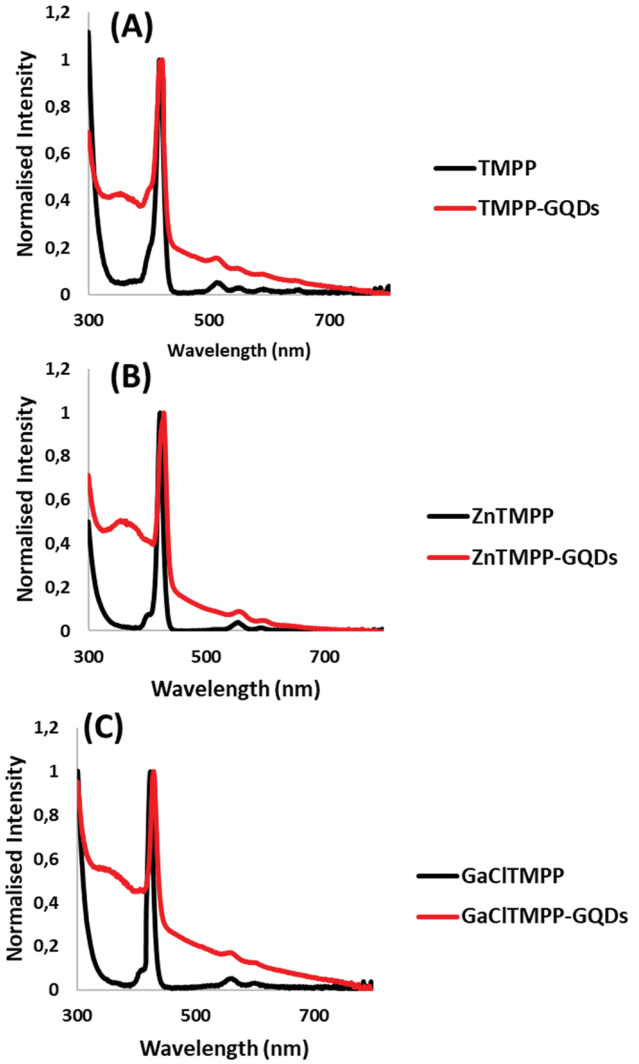

Fig. 1 Normalised electronic absorption spectra of (A) TMPP, (B) ZnTMPP and (C) GaClTMPP and porphyrin–GQD conjugates in DMF.

between 330 nm and 392 nm (Fig. 1); this peak has been associated with the π–π* transition of the sp^2 carbon electrons of the graphene core of GQDs as shown in the spectrum for GQDs, Fig. 2.[19,26] The four Q-bands of the metal-free precursor collapsed into two Q-bands following metalation, confirming the successful insertion of GaCl and Zn as a central metal.

The Soret bands of ZnTMPP, GaClTMPP, ZnTMPP–GQDs and GaClTMPP–GQDs were observed at 421 nm, 422 nm, 428 nm and 430 nm, respectively, Table 1. Red shifts were observed in the Soret bands following the insertion of the central metals. Red shifts have been reported[27] to be the result of the insertion of the central metal. Introduction of a heavy metal such as gallium and zinc could result in a degree of perturbation and electron delocalisation within the porphyrin macrocycle.[27] The GaClTMPP is red shifted as compared to ZnTMPP and this is due to the large size of gallium.

There were also red shifts observed in the Soret band between GaClTMPP and GaClTMPP–GQDs, and TMPP and

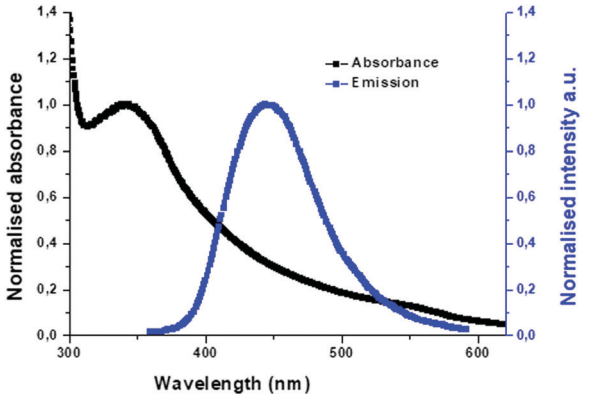

Fig. 2 Electronic absorption spectra and fluorescence emission spectra of GQDs. Excitation wavelength at 340 nm in DMF.

TMPP–GQDs as well as between ZnTMPP and ZnTMPP–GQDs. Red shifts have been observed in the porphyrin–graphene oxide nanoconjugates.[28] GQDs show typical broad absorption and narrow emission[19] with a fluorescence emission spectrum at 445 nm upon excitation at 340 nm. The GQDs were shown to be stable even when left in solution as no spectral changes were observed.

Fig. 3 shows the emission spectra of H_2 and Zn porphyrin and the porphyrin–GQD conjugates (as examples). The spectra of TMPP and ZnTMPP are typical[29] of porphyrins with two bands differing in intensity. The additional emission peak observed in the spectra is due to the GQDs. The decreases in the intensity of the low energy band of the porphyrins could be due to the presence of the GQDs.

Raman spectra

The quality of the as-synthesized GQDs and their nanoconjugates were confirmed by laser Raman spectral analysis, Fig. 4.

GQDs are known to exhibit the diagnostic Raman bands termed as the G and D bands resulting from the E_{2g} tangential vibrational mode of the sp^2 bonded carbons and the disordered A_{1g} breathing vibrational mode of the aromatic sp^2 carbon rings, respectively. The intensity ratio of the D band to the G band for the conjugates was calculated to be above 1 as shown in Fig. 4, which is an indication that porphyrin molecules successfully interacted with the GQDs by π–π stacking. The D : G ratio is generally considered as a good parameter for measuring the extent of functionalization of GQDs.

Dynamic light scattering

The sizes of the nanoconjugates were analysed using dynamic light scattering (DLS) measurements, Fig. 5.

The conjugates of GQDs with metal-free porphyrins have a smaller size as compared to the corresponding metallated derivatives, Fig. 5. It has been reported that central metals within the cavity of the porphyrins have the ability to change the hydrophobicity of the molecule.[30] The DLS sizes of TMPP–GQDs, ZnTMPP–GQDs and GaClTMPP–GQDs were determined to be 19.9 nm, 24.9 nm and 28.6 nm respectively, compared to GQDs alone at 10 nm, Table 1. DLS results show that there

Table 1 The photophysical parameters for the porphyrins and their conjugates with GQDs in DMF

Complexes[a]	λ_{Abs} (nm)	($\Phi_{F(GQDs)}$)	$\tau_{F(GQDs)}$ (ns)	($\Phi_{F(Porp)}$)	$\tau_{F(Porp)}$ (ns)	Eff	(Φ_{Δ}) ($\pm$ 0.01)
GQDs (10 nm)	343	0.35	6.1	—	—	—	—
TMPP	418	—	—	0.15	4.8	—	0.38
TMPP–GQDs (19.9 nm)	423	0.14	2.48	0.29	15.5	55	0.42
ZnTMPP	421	—	—	0.19	3.7	—	0.43
ZnTMPP–GQDs (24.9 nm)	428	0.09	1.96	0.26	8.9	71	0.49
GaClTMPP	422	—	—	0.05	3.1	—	0.44
GaClTMPP–GQDs (28.6 nm)	430	0.07	1.73	0.10	8.2	77	0.51

[a] Values in brackets are the DLS sizes in nm.

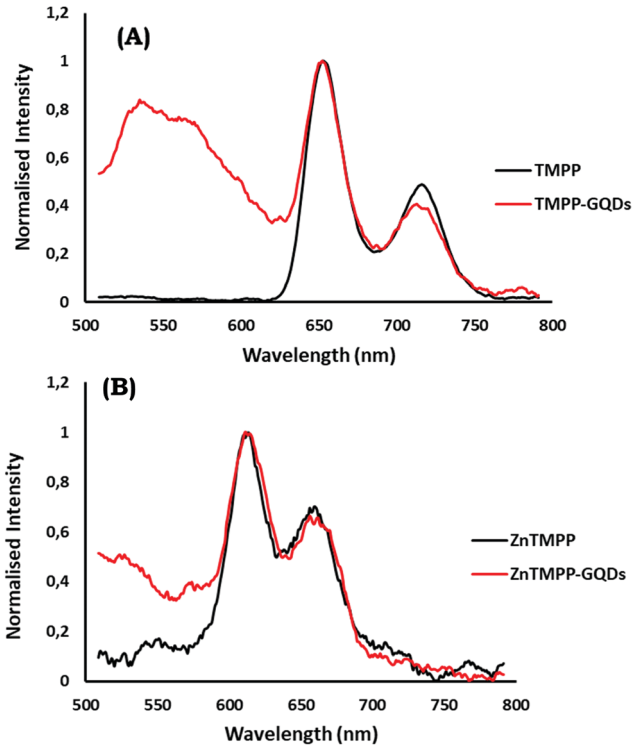

Fig. 3 Normalised fluorescence emission spectra of (A) TMPP and (B) ZnTMPP and porphyrin–GQD conjugates. Excitation λ = 490 nm in DMF.

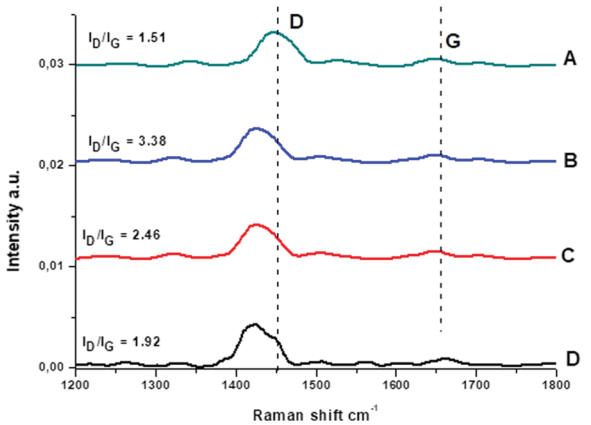

Fig. 4 Raman spectra of (A) GDQ, (B) TMPP–GQDs, (C) ZnTMPP–GQDs and (D) GaClTMPP–GQDs.

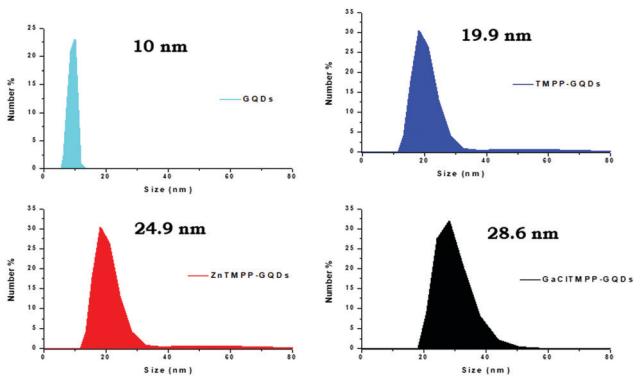

Fig. 5 Dynamic light scattering of GDQs, TMPP–GQDs, ZnTMPP–GQDs and GaClTMPP–GQDs 1% DMF.

was an increase in the sizes of the GQD nanoconjugates compared to the GQDs alone, which is also an indication of the formation of supramolecular assemblies of the GQDs and the porphyrins.

Transmission electron microscopy (TEM) images

Transmission electron microscopy (TEM) was used to determine the morphology and size distribution of the as-synthesized GQDs, Fig. 6.

The TEM images of the GQDs on their own show that the GQDs are monodispersed and the size ranges from 9–11 nm. The GQDs in the presence of porphyrins show aggregation. Porphyrins are known to show aggregation upon covalent and non-covalent interactions with the nanoparticles, due to the interaction between the porphyrins adsorbed onto adjacent nanoparticles. Aggregation by π–π stacking is common in porphyrins.[31]

Photophysical and photochemical parameters

Equations for the determination of fluorescence (Φ_F) and singlet oxygen (Φ_{Δ}) quantum yields may be found in the ESI.†

Fluorescence lifetimes (τ_f) and quantum yields (Φ_F)

The fluorescence lifetime (τ_f) of a complex defines the time a molecule spends in the excited state before returning to the ground state through fluorescence and it is directly related to the fluorescence quantum yield. The τ_f of all the complexes was determined using a time-correlated single photon count (TCSPC) method, following excitation at the emission maxima.

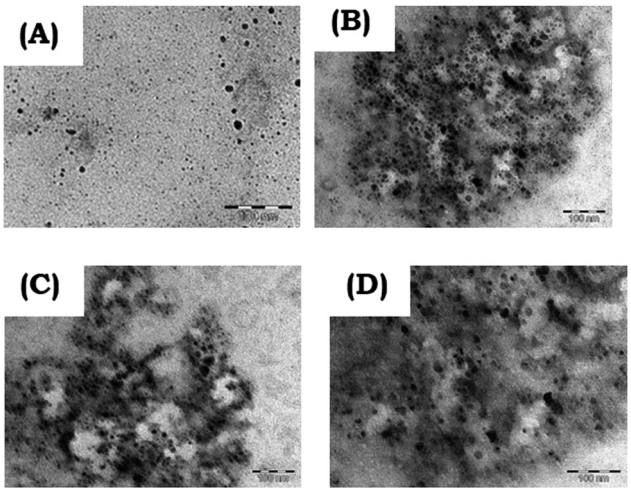

Fig. 6 Transmission electron micrographs of GQDs, TMPP–GQDs, ZnTMPP–GQDs and GaClTMPP–GQDs.

The fluorescence quantum yields (Φ_F) were determined by the comparative method, by comparing the fluorescence intensity of the complexes to that of ZnTPP standard where the porphyrin was excited and H_2SO_4 standard where the GQDs were excited. In Table 1, the Φ_F and τ_f are represented as $\Phi_{F(Porp)}$ and $\tau_{f(Porp)}$ when exciting where porphyrins absorb (490 nm), and $\Phi_{F(GQDs)}$ and $\tau_{f(GQDs)}$ when exciting where GQDs absorb (340 nm).

The quenching of the GQD emission by Zn 5,10,15,20-tetra(1-pyrenyl)porphyrin (ZnTPrP) has been reported,[32] and similar quenching was obtained in this work. The $\Phi_{F(GQDs)}$ went from 0.35 for GQDs alone to 0.14, 0.09 and 0.07 for the TMPP–GQDs, ZnTMPP–GQDs and GaClTMPP–GQDs, respectively, Table 1. The $\tau_{f(GQDs)}$ values also shortened for the GQDs in the presence of porphyrins. A typical fluorescence decay profile for the ZnTMPP–GQDs as an example is shown in Fig. 7. Mono-exponential decay profiles were obtained.

The quenching of the GQD emission may be due to Förster resonance energy transfer (FRET) and other processes that deactivate the excited state.[32] The decrease in $\Phi_{F(GQDs)}$ and τ_{GQDs} (when exciting where GQDs absorb) observed in Table 1 may be due to FRET.

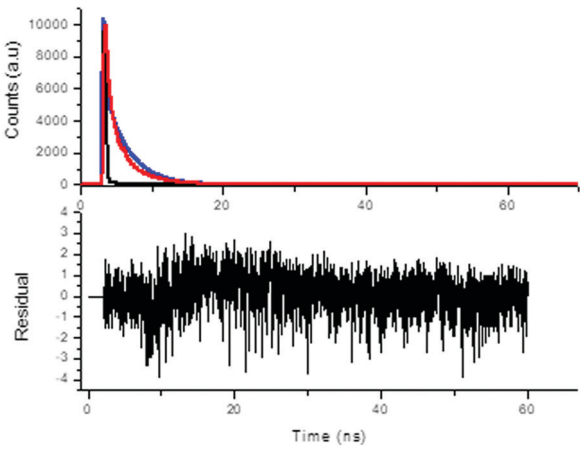

Fig. 7 Fluorescence decay profile of ZnTMPP–GQDS as an example in DMF.

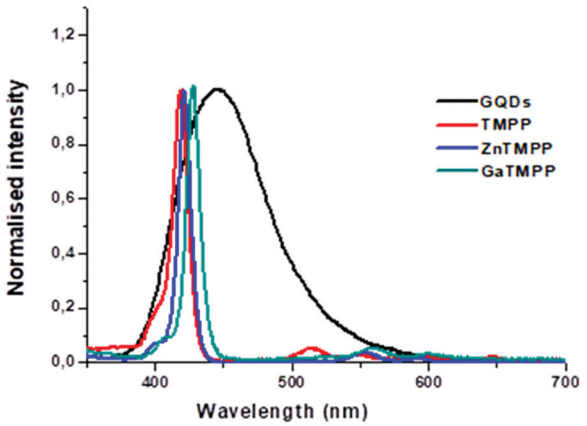

Fig. 8 Emission spectra of GQDs and absorption spectra of GaClTMPP. GQDs excitation at 340 nm in DMF.

FRET is a non-radiative energy transfer process which occurs between a photoexcited donor fluorophore upon the absorption of higher energy photons and an acceptor molecule in close proximity to the donor fluorophore.[32] FRET efficiency (Eff) was determined experimentally from the fluorescence quantum yields of the donor in the absence ($\Phi_{F(GQDs)}$) and presence ($\Phi^{conjugate}_{F(GQDs)}$) of the acceptor using eqn (1):[33]

$$\mathrm{Eff} = 1 - \frac{\Phi^{conjugate}_{F(GQDs)}}{\Phi_{F(GQDs)}} \quad (1)$$

FRET efficiencies were high for the GaClTMPP–GQD conjugates as compared to the other conjugates. This may be due to a more red-shifted Soret band compared to the other porphyrins, resulting in more overlap with GQD emission, Fig. 8.

FRET results from dipole–dipole interactions and is extremely dependent on the center-to-center separation distance between the donor and the acceptor (r), the degree of spectral overlap of the donor's fluorescence emission spectrum and the acceptor's absorption spectrum[34,35] as shown in Fig. 8.

Singlet oxygen quantum yield (Φ_Δ)

Singlet oxygen is the major cytotoxic species responsible for the cancer cell death in PDT. The Φ_Δ were determined to be 0.38, 0.42, 0.43, 0.49, 0.44 and 0.51 for the TMPP, TMPP–GQDs, ZnTMPP, ZnTMPP–GQDs, GaClTMPP and GaClTMPP–GQDs respectively. Diamagnetic metals such as zinc and gallium have been shown to have high triplet and singlet oxygen quantum yields, and long triplet lifetimes which are essential for the photosensitization process.[36] The electron-donating groups are known to increase intersystem crossing (ISC) in porphyrins,[37] hence the presence of GQDs in the conjugates increases ISC, resulting in improved Φ_Δ values of the porphyrins in the presence of GQDs.

MCF-7 breast cancer cell studies

***In vitro* dark toxicity.** The dark toxicity studies of the molecules were performed at 5, 10, 20, 40, 80 and 120 μg ml^{-1}, Fig. 9. At all concentrations, the cell viability percentages

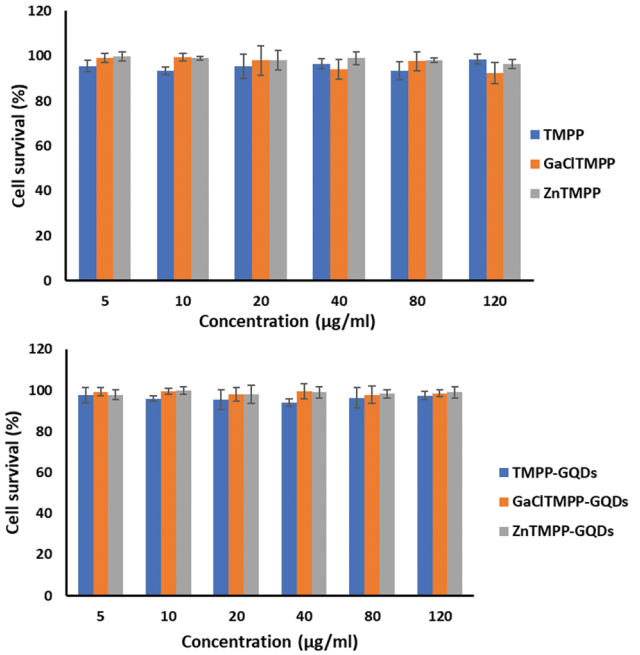

Fig. 9 Dark toxicity plots for porphyrins and their conjugates at 5, 10, 20, 40, 80 and 120 μg ml^{-1}.

were all above 90%. *In vitro* dark toxicity is undesirable for photosensitizers aimed for use in PDT. The dark toxicity of the photosensitizers was determined in 1% DMSO which was used as the stock diluent. DMSO (1%) used had a negligible effect on the cells seen in this work and this has also been reported.[38–40]

Upon analysis of the triplicate replicate data of each concentration, we observed no statistically significant difference as the *p*-value was found to be greater than 0.05.

Photodynamic therapy. The photo-irradiations were performed using a 420 nm LED and the irradiation time was 300 s. The absorbance of the 96-well plates was measured at an excitation wavelength of 450 nm using a Synergy 2 multimode microplate reader (BioTek1). There were no changes in the spectra of the porphyrins following irradiation for the PDT studies, hence confirming the stability. The phototoxicity of TMPP, TMPP–GQDs, ZnTMPP, ZnTMPP–GQDs, GaClTMPP and GaClTMPP–GQDs against MCF-7 breast cancer increased upon irradiation and increased with increase in concentration. As the concentration increased, the cell viability decreased, Fig. 10.

The GaClTMPP–GQDs showed higher phototoxicity at 15% cell viability as compared to the TMPP, TMPP–GQDs, ZnTMPP, ZnTMPP–GQDs and GaClTMPP at 120 μg ml^{-1}. An increase in PDT activities were observed for the porphyrins in the presence of GQDs.

In PDT, an excited triplet state of the photosensitizer transfers its energy to the ground state molecular oxygen resulting in the production of singlet oxygen which is the main cytotoxic species in PDT. Thus, the PDT activity is expected to follow the same trend as the singlet oxygen quantum yields which was evident in this work, Fig. 10.

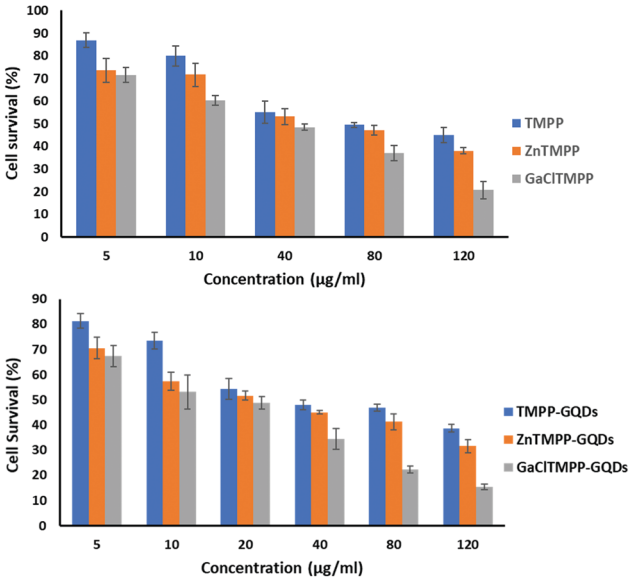

Fig. 10 PDT for porphyrins and their conjugates at 5, 10, 20, 40, 80 and 120 μg ml^{-1} and 40 J cm^{-2}.

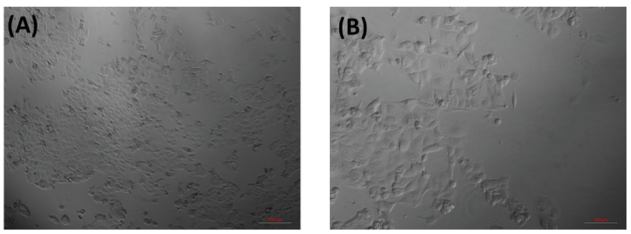

Fig. 11 PDT micrographs of MCF7 breast cancer cells of (A) GaClTMPP and (B) GaClTMPP–GQDs.

Fig. 11 shows the PDT micrographs of the MCF7 breast cancer cells of (A) GaClTMPP and (B) GaClTMPP–GQDs when irradiated at 40 J cm^{-2}. The difference in the presence of the GQDs can be seen in Fig. 11(B) where more cell death occurred.

$^{*}P < 0.05$, is considered to be a statistically significant difference. We observed a statistically significant difference as the concentration increased. There was a significant difference between the dark toxicity and the PDT data for all complexes.

Conclusions

Porphyrins and GQDs have been interacted through π–π interaction to enhance the photophysical properties. Different spectroscopic techniques were used to characterize the nanocomposites and the interaction mechanism. Fluorescence and singlet oxygen quantum yields improved for porphyrins in the presence of GQDs, which also improved the PDT activities. Low dark toxicity of the nanocomposites was observed which indicated high promising application in PDT.

Conflicts of interest

There are no conflicts to declare.

Acknowledgements

This work was supported by the Department of Science and Technology (DST)/Nanotechnology (NIC) and National Research Foundation (NRF) of South Africa through DST/NRF South African Research Chairs Initiative for Professor of Medicinal Chemistry and Nanotechnology (UID 62620) and Rhodes University.

Notes and references

1 J. Ge, M. Lan, B. Zhou, W. Liu, L. Guo, H. Wang, Q. Jia, G. Niu, X. Huang, H. Zhou, X. Meng, P. Wang, C. S. Lee, W. Zhang and X. Han, *Nat. Commun.*, 2014, **5**, 1–8.
2 E. J. G. J. Dolmans, D. Fukumura and P. K. Jain, *Nat. Rev. Cancer*, 2013, **3**, 380–387.
3 A. P. Castano, P. Mroz and M. R. Hamblin, *Nat. Rev. Cancer*, 2006, **6**, 535–545.
4 C. M. Moore, D. Pendse and M. Emberton, *Nat. Clin. Pract. Urol.*, 2009, **6**, 18–30.
5 R. Matshitse, N. Nwaji, M. Managa, E. Prinsloo and T. Nyokong, *J. Photochem. Photobiol., A*, 2018, **367**, 253–260.
6 R. Pandey and G. Zheng, in *The Porphyrin Handbook*, ed. K. M. Kadish, K. M. Smith and R. Guilard, Academic Press, 2000, vol. 6.
7 E. Dube, D. O. Oluwole, E. Prinsloo and T. Nyokong, *New J. Chem.*, 2018, **42**, 10214–10225.
8 R. Bonnett, *Chemical Aspects of Photodynamic Therapy*, Gordon and Breach Science Publishers, Amsterdam, 2000.
9 J. Kou, D. Dou and L. Yang, *Oncotarget*, 2017, **8**, 81591–81603.
10 Y. Cao, H. Dong, Z. Yang, X. Zhong, Y. Chen, W. Dai and X. Zhang, *ACS Appl. Mater. Interfaces*, 2017, **9**, 159–166.
11 D. M. Guldi, *Chem. Soc. Rev.*, 2002, **31**, 22–36.
12 M. Ethirajan, Y. Chen, P. Joshi and R. K. Pandey, *Chem. Soc. Rev.*, 2011, **40**, 340–362.
13 U. S. Chung, J. H. Kim, B. Kim, E. Kim, W. D. Jang and W. G. Koh, *Chem. Commun.*, 2016, **52**, 1258–1261.
14 J. Liu, Y. Yang, W. Zhu, X. Yi, Z. Dong, X. Xu, M. Chen, K. Yang, G. Lu, L. Jiang and Z. Liu, *Biomaterials*, 2016, **97**, 1–9.
15 A. E. O'Connor, W. M. Gallagher and A. T. Byrne, *Photochem. Photobiol.*, 2009, **85**, 1053–1074.
16 L. Li, G. Wu, G. Yang, J. Peng, J. Zhao and J. Zhu, *Nanoscale*, 2013, **5**, 4015–4039.
17 S. Benitez-Martinez and M. Valcarel, *TrAC, Trends Anal. Chem.*, 2015, **72**, 93–113.
18 Z. Fan, S. Li, F. Yuan and L. Fan, *RSC Adv.*, 2015, **5**, 19773–19789.
19 M. Managa, O. J. Achadu and T. Nyokong, *Dyes Pigm.*, 2018, **148**, 405–416.
20 D. Qu, M. Zheng, P. Du, Y. Zhou, L. Zhang, D. Li, H. Tan, Z. Zhao and Z. Xied, *Nanoscale*, 2013, **5**, 12272–12277.
21 J. Ge, L. Minhuan, B. Zhou, W. Liu, L. Guo, H. Wang, Q. Jia, G. Niu, X. Huang, H. Zhou, M. Xiangmin, W. Pengfei, L. Chun-Sing, W. Zhang and X. Han, *Nat. Commun.*, 2014, **5**, 4596–4603.
22 D. D. La, A. Rananaware, M. Salimimarand and S. V. Bhosale, *ChemistrySelect*, 2016, **1**, 4430–4434.
23 O. J. Achadu, I. Uddin and T. Nyokong, *Photochem Photobiol A.*, 2016, **317**, 12–25.
24 M. Gouterman, in *The Porphyrins, Part A. Physical Chemistry*, ed. D. Dolphin, Academic Press, New York, 1978, vol. 3.
25 K. M. Smith, *Porphyrins and Metalloporphyrins*, Elsevier, Amsterdam, 1975.
26 C. K. Chua, Z. Sofer, P. Šimek, O. Jankovský, K. KlÍmová, S. Bakardjieva, S. H. Kučková and M. Pumera, *ACS Nano*, 2015, **9**, 2548–2555.
27 R. Giovannetti, The Use of Spectrophotometry UV-Vis for the Study of Porphyrins, in *Macro To Nano Spectroscopy*, ed. J. Uddin, Intech, Open Science, 2012.
28 Z. D. Liu, H. X. Zhao and C. Z. Huang, *PLoS One*, 2012, **7**, 50367, DOI: 10.1371/journal.pone.0050367.
29 M. Uttamlal and A. S. Holmes-Smith, *Chem. Phys. Lett.*, 2008, **454**, 223–228.
30 A. C. Wenceslau, G. L. Q. C. Ferreira, N. Hioka and W. Caetano, *J. Porphyrins Phthalocyanines*, 2015, **19**, 1168–1176.
31 K. Kano, K. Fukuda, H. Wakami, R. Nishiyabu and R. F. Pasternack, *J. Am. Chem. Soc.*, 2000, **122**, 7494–7502.
32 O. J. Achadu, M. Managa and T. Nyokong, *J. Photochem. Photobiol., A*, 2017, **333**, 174–185.
33 C. Berney and G. Danuser, *Biophys. J.*, 2003, **84**, 3992–4010.
34 J. R. Lakowicz, *Principles of Fluorescence Spectroscopy*, Kluwer Academic, New York, 2nd edn, 1999, p. 35.
35 B. Valeur, *Molecular Fluorescence: Principles and Applications*, Wiley-VCH, Weinheim, Germany, 2001.
36 D. O. Oluwole, E. Prinsloo and T. Nyokong, *Polyhedron*, 2016, **119**, 434–444.
37 T. G. B. de Souza, M. G. Vivas, C. R. Mendonça, S. Plunkett, M. A. Filatov, M. O. Senge and L. De Boni, *J. Porphyrins Phthalocyanines*, 2016, **20**, 282–291.
38 A. Boire, L. Covic, A. Agarwa, S. Jacques, S. Sherifi and A. Kuliopulos, *Cell*, 2005, **120**, 303–313.
39 R. O. Ogbodu, J. L. Limson, E. Prinsloo and T. Nyokong, *Synth. Met.*, 2015, **204**, 122–132.
40 M. Managa, J. Britton, E. Prinsloo and T. Nyokong, *Polyhedron*, 2018, **152**, 102–107.

